JOURNAL OF GUIDANCE, CONTROL, AND DYNAMICS
Vol. 26, No. 4, July–August 2003

Optimal Strategy for Geostationary Orbit Acquisition Using Ion Propulsion

Christian Circi*
University of Rome "La Sapienza," 00184 Rome, Italy

The geostationary satellite for telecommunication, Artemis, is equipped with a chemical propulsion system and an ion propulsion system. Because of the third-stage ignition failure of the Ariane V launcher, the low-thrust propulsion system is used to complete the transfer orbit to geostationary Earth orbit. The optimal trajectory is determined using Pontryagin's principle. All constraints for the thrust direction, due to the initial design and onboard breakdown, are considered in the optimization process, and the minimum-time problem is solved. The effect of perturbations, namely, the gravitational force of the sun and the moon, the oblateness and triaxiality of the Earth, and the solar radiation pressure, are considered. The performances of the transfer orbit and the optimal thrust strategy are presented for every case. The transfer time, considering the perturbations, increases by 20 days with respect to the Keplerian case, but this does not imply an increase in propellant mass consumption. Finally a comparison with a solution obtained using a parametric optimization process is given. The parametric optimization results are close to those of the Pontryagin solution, but do not allow the satellite to obtain the best transfer time. In fact, the control strategy efficiency depends on the number of variables used in the process, and a time-variable strategy is possible only with an enormous increase of the computational effort, although it is natural when the Pontryagin principle is applied.

Introduction

THE optimal low-thrust and the combined chemical–low-thrust transfer problems have been studied by many authors.[1–8] Recently ESA has become interested in missions that foresee the use of low-thrust engines, which make significant propellant savings possible.[9,10] The failure of the Ariane V launcher resulted in delivering the geostationary satellite for telecommunication, Artemis, into an orbit far from the desired geostationary transfer orbit (GTO). After a series of impulsive maneuvers, carried out using the chemical engine, the satellite reached an orbit close to the geostationary orbit (GEO). This paper studies the possibility of bringing the satellite onto the GEO, using only the ion propulsion system. The minimum-time problem is solved by applying the Pontryagin principle due to its flexibility when considering different types of constraints.[11,12] The initial Artemis orbital parameters refer to the epoch 6 September 2001, but the proposed procedure is independent of the initial date.

The problem is first studied using the Keplerian model. Then, once the importance of the perturbation effect has been revealed, the J_2 effect is introduced, and then the other perturbations are added. Because of the consequent complexity, when the effect of all perturbations is considered, the Lagrange multipliers system is simplified by omitting the derivatives of the perturbations with respect to the state. This simplification is also applied to the case where only the J_2 perturbation is taken into consideration, and the result is compared with the one obtained with no simplification.

In the last part of the work, the transfer trajectory is determined using a parametric optimization technique, in which the amplitude of the thrust arcs is used as a parameter. Results are compared to those obtained using the Pontryagin principle.

Artemis Satellite Mission

Because of a malfunction of the Ariane V launcher, the Artemis spacecraft was placed into an orbit $6970 \times 23{,}896$ km with an inclination of approximately 3 deg, vs the nominal value $7235 \times 42{,}215$ km and 2 deg of inclination (GTO). In a sequence of maneuvers using the chemical propulsion system, an intermediate orbit was reached that was quasi circular and almost equatorial (Table 1). The mass budget on 6 Septemeber 2001 was dry mass 1535 kg, liquid mass 55 kg, and Xenon mass 44 kg (total mass 1634 kg). Artemis is equipped with two independent ion propulsion branches, the electron bombardment ion thruster assembly (EITA) and the radio frequency ion thruster assembly (RITA). Each branch consists of two thruster units (Fig. 1).

1) EITA, made by Marta-UK, delivers 18 mN of thrust at an I_{sp} of 3000 s. The units are mounted on the $-Z$ face of the spacecraft, which normally faces away from the Earth, and at an angle of 49.86 deg with respect to the y axis. Therefore, the nominal thrust angle is 40.14 deg from the orbit plane. An additional rotation of 3 deg with respect to the Z axis is possible.

2) RITA, made by EADS, delivers 15 mN of thrust, also at an I_{sp} of 3000 s. The units are mounted in a similar fashion to the EITAs, but at an angle of 43.6 deg with respect to the y axis.

The thrusters, nominally foreseen only for north–south station-keeping maneuvers, are used as the propulsion system in the transfer orbit. Because of their mounting and onboard breakdown, the Z axis is constrained to remain coincident with the velocity vector and the Y axis perpendicular to the radial direction.

Optimal Solution for Keplerian Case

The dynamic model is described by a system of differential equations with fixed initial and final conditions, and the minimum-time problem is studied using the Pontryagin principle.[11,13,14] The equations of motion are written in the r, ϑ, h body system (respectively, radial, transverse, and normal direction) and in terms of the acceleration components A_R, A_T, and A_W. The state vector is expressed in terms of equinoctial elements $(a, P_1, P_2, Q_1, Q_2, l)$, nonsingular for the GEO[15–21] and related to the classical elements by $a = a$, $P_1 = e\sin(\omega + \Omega)$, $P_2 = e\cos(\omega + \Omega)$, $Q_1 = \tan(i/2)\sin(\Omega)$, $Q_2 = \tan(i/2)\cos(\Omega)$, and $l = (\omega + \Omega) + M$. In these variables, the equations of motion become

$$\frac{da}{dt} = \frac{2a^2}{\sqrt{\mu a(1-e^2)}}\left\{[P_2\sin(L) - P_1\cos(L)]A_R + \frac{p}{r}A_T\right\}$$

Received 2 April 2002; revision received 15 January 2003; accepted for publication 20 January 2003.

*Assistant Professor, Scuola di Ingegneria Aerospaziale, Department of Aerospace and Astronautics Engineering, v. Eudossiana 18.

Table 1 Orbital elements on 6 September 2001

Parameter	Value
Date	6 September 2001 00:00:00
Semimajor axis, km	37,306.653315
Eccentricity	0.000827
Inclination, deg	0.870949
RAAN, deg	156.410374
Argument of perigee, deg	9.099137
True anomaly, deg	61.133779

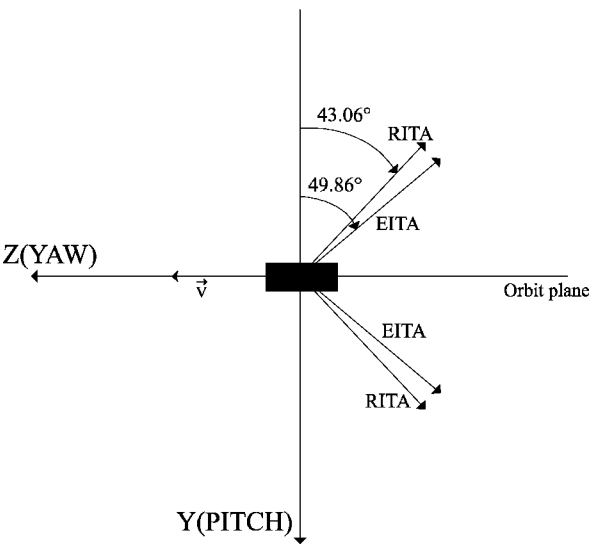

Fig. 1 Geometry for the EITA and RITA propulsion systems.

$$\frac{\mathrm{d}P_1}{\mathrm{d}t} = \frac{r}{h}\left\{-\frac{p}{r}\cos(L)A_R + \left[P_1 + \left(1+\frac{p}{r}\right)\sin(L)\right]A_T - P_2[Q_1\cos(L) - Q_2\sin(L)]A_W\right\}$$

$$\frac{\mathrm{d}P_2}{\mathrm{d}t} = \frac{r}{h}\left\{\frac{p}{r}\sin(L)A_R + \left[P_2 + \left(1+\frac{p}{r}\right)\cos(L)\right]A_T + P_1[Q_1\cos(L) - Q_2\sin(L)]A_W\right\}$$

$$\frac{\mathrm{d}Q_1}{\mathrm{d}t} = \frac{r}{2h}\left(1+Q_1^2+Q_2^2\right)\sin(L)A_W$$

$$\frac{\mathrm{d}Q_2}{\mathrm{d}t} = \frac{r}{2h}\left(1+Q_1^2+Q_2^2\right)\cos(L)A_W$$

$$\frac{\mathrm{d}l}{\mathrm{d}t} = n - \frac{r}{h}\left\{\left[\frac{a}{a+a\sqrt{1-P_1^2-P_2^2}}\left(\frac{p}{r}\right)[P_1\sin(L)+P_2\cos(L)] + \frac{2a\sqrt{1-P_1^2-P_2^2}}{a}\right]A_R + \frac{a}{a+a\sqrt{1-P_1^2-P_2^2}}\left(1+\frac{p}{r}\right) \times [P_1\cos(L) - P_2\sin(L)]A_T + [Q_1\cos(L) - Q_2\sin(L)]A_W\right\} \tag{1}$$

where

L = true longitude, $(\omega+\Omega)+f$
n = mean motion, $\sqrt{(\mu/a^3)}$
A_R = radial component of thrust acceleration
A_T = transverse component of thrust acceleration
A_W = normal component of thrust acceleration

After the linearization with respect to the GEO orbit and with $\mathrm{d}t/na = \mathrm{d}s$, the system for the state variables is

$$\frac{\mathrm{d}a}{\mathrm{d}s} = 2aA_T, \qquad \frac{\mathrm{d}P_1}{\mathrm{d}s} = 2\sin(L)A_T, \qquad \frac{\mathrm{d}P_2}{\mathrm{d}s} = 2\cos(L)A_T$$

$$\frac{\mathrm{d}Q_1}{\mathrm{d}s} = \sin(L)\frac{A_W}{2}, \qquad \frac{\mathrm{d}Q_2}{\mathrm{d}s} = \cos(L)\frac{A_W}{2}, \qquad \frac{\mathrm{d}L}{\mathrm{d}s} = \frac{\mu}{a^2} \tag{2}$$

The Hamiltonian of this system is written as $H = \lambda_z^T \dot{z}$, where $\boldsymbol{\lambda}_z^T = (\lambda_a, \lambda_{P_1}, \lambda_{P_2}, \lambda_{Q_1}, \lambda_{Q_2}, \lambda_L)$ is the vector of Lagrange multipliers adjoint to the state variable $\boldsymbol{z} = (a, P_1, P_2, Q_1, Q_2, L)^T$ and the Euler–Lagrange equations are given by $\dot{\lambda}_z = -\partial H/\partial z$. We minimize the total transfer time, and the performance index is

$$J = \int_{t_0}^{t_f} \mathrm{d}t$$

For an admissible solution, a necessary condition for optimality is that there exists a nonzero continuous vector function $\boldsymbol{z} = (a, P_1, P_2, Q_1, Q_2, L)^T$, such that for all t, $t_0 \le t \le t_f$, the function H attains a minimum at the point $u = u(t)$, the Hamiltonian function is constant with $H \le 0$, and the Euler–Lagrange equations are satisfied (see Ref. 11). Thus, for the optimal control problem, it is necessary to find the initial values of the Lagrange multipliers λ that result in meeting the final state. Moreover, the control law $u(t)$ must satisfy the first and second necessary conditions of the Pontryagin theorem.

In this case the Hamiltonian function is

$$H = \left[2a\lambda_a + 2\sin(L)\lambda_{P_1} + 2\cos(L)\lambda_{P_2}\right]A_T + \left[\sin(L)\lambda_{Q_1} + \cos(L)\lambda_{Q_2}\right](A_W/2) + \lambda_L(\mu/a^2) \tag{3}$$

When A_T and A_W are written as

$$A_T = (A_N + A_S)K_G, \qquad A_W = (A_N - A_S)K \tag{4}$$

where A_N and A_S are integer values (0 or 1), and when K_G is the modulus of the tangential thrust component and K the modulus of the normal thrust component, the Hamiltonian function becomes

$$H = \left[2a\lambda_a + 2\sin(L)\lambda_{P_1} + 2\cos(L)\lambda_{P_2}\right](A_N + A_S)K_G + \left[\sin(L)\lambda_{Q_1} + \cos(L)\lambda_{Q_2}\right](A_N - A_S)(K/2) + \lambda_L(\mu/a^2) \tag{5}$$

For the Lagrange multipliers equations, we obtain

$$\lambda_a' = -2\lambda_a(A_N + A_S)K_G + \left(2\mu\lambda_L/a^3\right)$$

$$\lambda_{P_1}' = 0, \qquad \lambda_{P2}' = 0, \qquad \lambda_{Q_1}' = 0, \qquad \lambda_{Q2}' = 0$$

$$\lambda_L' = -\left[2\cos(L)\lambda_{P_1} - 2\sin(L)\lambda_{P_2}\right](A_N + A_S)K_G - \left[\cos(L)\lambda_{Q_1} - \sin(L)\lambda_{Q_2}\right](A_N - A_S)(K/2) \tag{6}$$

The first necessary condition for the Pontryagin principle is that the Hamiltonian function is minimal at each point. Because the EITA and RITA engines cannot be used at the same time, we have only four possible configurations for the control (Fig. 2): no thrust (0), thrust with north (N) or south (S) component, and thrust with both components (N+S). The Hamiltonian function attains its minimum

only on the boundary of the polyhedron (0, N, S, S+N). Every thrust configuration corresponds to specific values for A_N and A_S; in particular, the no-thrust case (0) corresponds to $A_N = 0$, $A_S = 0$; the case with only an N component corresponds to $A_N = 1$, $A_S = 0$; the case with only an S component corresponds to $A_N = 0$, $A_S = 1$; and the case with N+S components corresponds to $A_N = 1$, $A_S = 1$. The minimum Hamiltonian value determines the values for A_N and A_S as functions of time and, thus, the optimal control strategy.

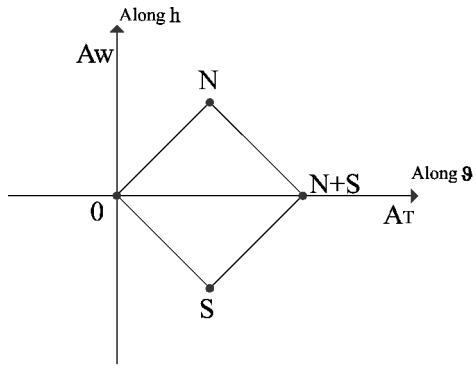

Fig. 2 Configuration for the control.

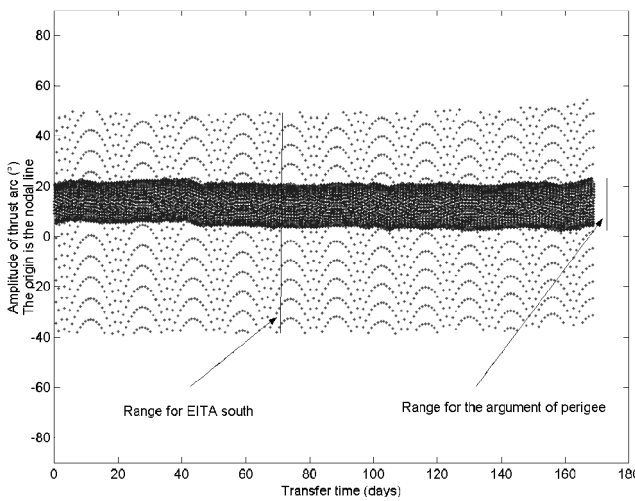

Fig. 3 Optimal thrust strategy for EITA S: Keplerian case.

The results obtained for the minimum-time problem show that the optimal solution uses only the EITA engine at the minimum possible angle with respect to the Z axis (37.14 deg). The performances are presented in terms of transfer time (days), final eccentricity, final inclination, and optimal thrust strategy (Table 2). For the optimal thrust strategy, the amplitude of the thrust arc is indicated. (The origin is the nodal line.) On the ascending node, the EITA engine with the S component is used; for the descending node, the EITA engine with the N component is used, and on the remaining arcs the EITA engine with N+S components is used.

The thrusters for inclination change are operative for about 90 deg of true anomaly, but these angles do not remain central with respect to the nodal line. Figure 3 plots the control strategy for the EITA S engine; in particular, the dots indicate the region where the EITA S is active. The strategy is indicated with respect to the ascending node, and so the origin (0 deg) is the nodal line. We can see that the thrust with the EITA S begins about 40 deg before the nodal line and finishes about 50 deg after the nodal line. This range remains quasi constant during the transfer. A similar behavior is valid for the EITA N engine at the descending node (Fig. 4). In Fig. 3 we can also see the variation of the argument of perigee during the transfer (central band). The perigee remains near the nodal line, so that the thrust for inclination changes (EITA S and EITA N) is applied in a high-efficiency area for this type of maneuver (Fig. 4). Note that, for the minimum transfer time orbit, the semi-axis and the inclination must reach the geostationary values at the same time. In fact, we have two possibilities: The first is that the satellite reaches the geostationary value for the semi-axis before the inclination. In this case, the geometry of the propulsion system cannot permit the satellite to change its inclination without increasing again the semi-axis. When the inclination reaches the zero value, the final semi-axis is bigger than the geostationary value, and so we must discard this eventuality. The second possibility is that the inclination reaches the zero value before the semi-axis reaches the geostationary value. This case is acceptable because the thrust with EITA with N and S components does not change the inclination and the geostationary

Table 2 Optimal Keplerian case results

Parameter	Value
Amplitude ascending node thrust, deg	−40, +50
Amplitude descending node thrust, deg	−40, +50
Inclination, deg	0.0086
Transfer time, days	169.9
Eccentricity	0.00007
Expended mass, kg	13.4

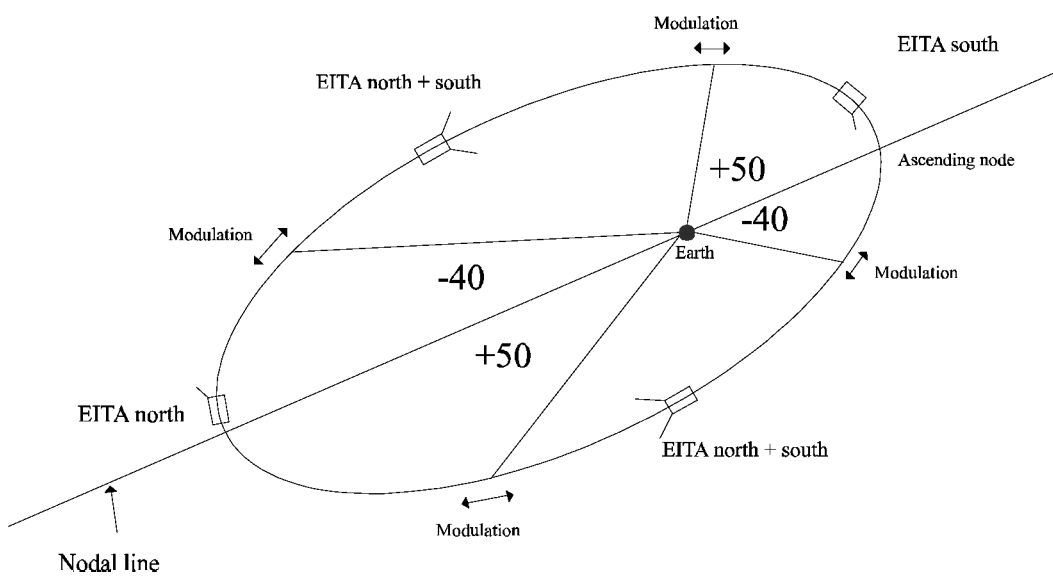

Fig. 4 Thrust strategy for the transfer orbit.

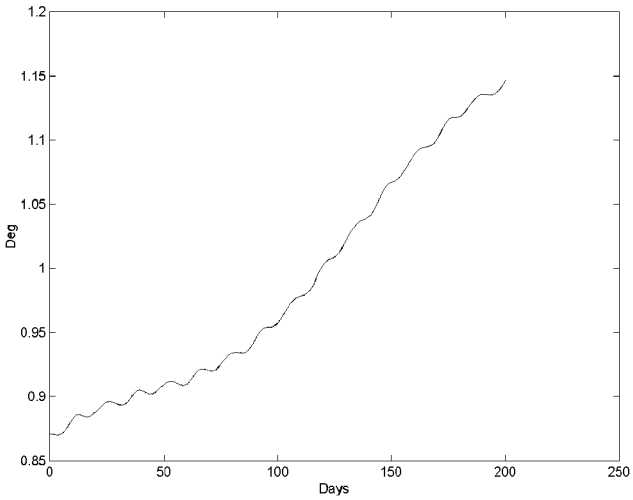

Fig. 5 Natural evolution of inclination.

values can be met. A limit case of this second possibility is that the geostationary values of semi-axis and inclination are reached at the same time. Numerical simulation reveals that this limit case is the best for the minimum-time transfer trajectory.

Natural Evolution of Intermediate Orbit

The preceding solution, carried out in a Keplerian model, gave about 170 days for the transfer time. This long period involves the study of the influence of the perturbation forces for the Artemis orbit. The natural evolution of the orbital elements is studied taking into account 1) the sun and moon gravitational effect, 2) earth oblateness and triaxiality, and 3) solar radiation pressure. The orbital state is numerically propagated for a period of 200 days and the initial orbital elements, in the Mean Equatorial Earth 2000 (MEE2000) reference frame, are shown in Table 1.

The result of the simulation indicates that the effect on the inclination, due primarily to third-body forces, is not negligible (Fig. 5). This is an important parameter for GEO. Therefore, the perturbation effects must be included in the optimization process.

Optimal Solution Including the J_2 Harmonic Effect

In the reference frame, the perturbation forces appear with a tangential, normal, and perpendicular acceleration. When the acceleration due to the J_2 perturbation is computed numerically and added to the thrust acceleration, the equations of motion become

$$\frac{\mathrm{d}a}{\mathrm{d}s} = 2aA_T, \qquad \frac{\mathrm{d}P_1}{\mathrm{d}s} = 2\sin(L)A_T - \cos(L)A_R$$

$$\frac{\mathrm{d}P_2}{\mathrm{d}s} = 2\cos(L)A_T + \sin(L)A_R, \qquad \frac{\mathrm{d}Q_1}{\mathrm{d}s} = \sin(L)\frac{A_W}{2}$$

$$\frac{\mathrm{d}Q_2}{\mathrm{d}s} = \cos(L)\frac{A_W}{2}, \qquad \frac{\mathrm{d}L}{\mathrm{d}s} = -2A_S + \frac{\mu}{a^2} \tag{7}$$

where A_R, A_T, and A_W include the engine thrust and the J_2 acceleration.

In the Hamiltonian function we can separate the contribution of the thrust acceleration (A_{TM}, A_{WM}) from the contribution due to J_2 (A_{RJ_2}, A_{TJ_2}, A_{WJ_2}):

$$H = \left[2a\lambda_a + 2\sin(L)\lambda_{P_1} + 2\cos(L)\lambda_{P_2}\right]\left(A_{TM} + A_{TJ_2}\right) + \left[\sin(L)\lambda_{Q_1} + \cos(L)\lambda_{Q_2}\right]\tfrac{1}{2}\left(A_{WM} + A_{WJ_2}\right) + \left[-\cos(L)\lambda_{P_1} + \sin(L)\lambda_{P_2} - 2\lambda_L\right]A_{RJ_2} + (\mu/a^2)\lambda_L \tag{8}$$

For the multipliers equations, the system is complex (see the Appendix), but after the linearization with respect to the GEO orbit, only the contribution of the derivative $\partial A_{RJ_2}/\partial a$ remains[22]:

$$\frac{\partial A_{RJ_2}}{\partial a} = -\frac{3\mu m R_e J_2}{4}\left(-\frac{4}{a^5}\right) \tag{9}$$

and the system becomes

$$\lambda'_a = -\left\{2\lambda_a A_{TM} + \left[-\cos(L)\lambda_{P_1} + \sin(L)\lambda_{P_2} - 2\lambda_a\right] \times \frac{\partial A_{RJ_2}}{\partial a} - \frac{2\mu\lambda_L}{a^3}\right\}$$

$$\lambda'_{P_1} = 0, \qquad \lambda'_{P2} = 0, \qquad \lambda'_{Q_1} = 0, \qquad \lambda'_{Q2} = 0$$

$$\lambda'_L = -\left\{\left[2\cos(L)\lambda_{P_1} - 2\sin(L)\lambda_{P_2}\right]A_{TM} + \left[\cos(L)\lambda_{Q_1} - \sin(L)\lambda_{Q_2}\right]\frac{A_{WM}}{2} + \left[\sin(L)\lambda_{P_1} + \cos(L)\lambda_{P_2}\right]A_{RJ_2}\right\} \tag{10}$$

We can find a strategy that satisfies the first and the second necessary conditions of the Pontryagin theorem. The performances are given in Table 3, and the thrust angle strategy for the EITA S engine is shown in Fig. 6. For the EITA N engine, we have the same behavior. The solution is similar to the Keplerian case. The amplitude of the thrust arc, for change of inclination (EITA S and EITA N), increases by only 5 deg (from 90 to 95 deg). In fact, the most important perturbation, in this case, depends principally on the luni–solar effect and not on J_2 (or the solar pressure).

Note that in the last part of the transfer, the rotation of the argument of perigee is followed by the same rotation of the thrust arc for the EITA S engine (Fig. 6). The thrust strategy, to change the inclination, takes into consideration the rotation of perigee, and the optimal geometry is a combination between the thrust centered on the nodal line and the argument of perigee.

Table 3 Optimal Keplerian $+J_2$ case results

Parameter	Value
Amplitude ascending node thrust, deg	−36, +59
Amplitude descending node thrust, deg	−36, +62
Inclination, deg	0.0078
Transfer time, days	170.9
Eccentricity	0.00007
Expended mass, kg	13.4

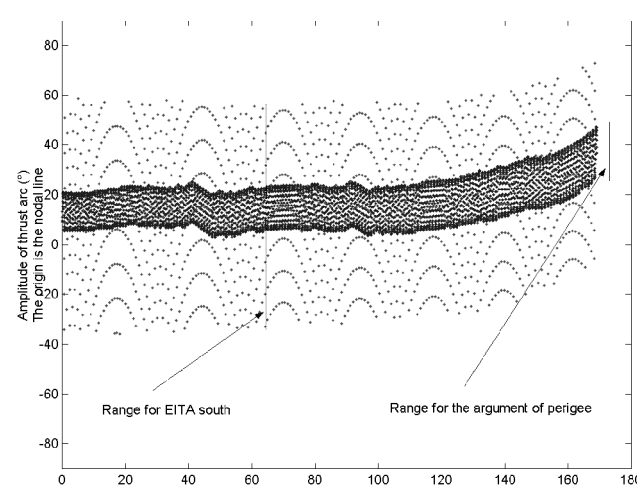

Fig. 6 Optimal thrust strategy for EITA S: Keplerian $+J_2$ case.

The consumption of propellant is practically the same. In fact, the transfer time increases by only one day and the thrust (only 18 mN) cannot produce a significant change. Moreover, the satellite takes more time, with respect to the Keplerian case, using the engines with only one component (EITA S and EITA N).

Optimization Process Including All Perturbation Forces

We now consider all of the perturbation forces (J_2, luni–solar, and radiation pressure) in the optimization process. The Hamiltonian function is

$$H = \left[2a\lambda_a + 2\sin(L)\lambda_{P_1} + 2\cos(L)\lambda_{P_2}\right][(A_N + A_S)K_G + A_{T\_\text{pert}}] + \left[\sin(L)\lambda_{Q_1} + \cos(L)\lambda_{Q_2}\right]\tfrac{1}{2}[(A_N - A_S)K + A_{W\_\text{pert}}] + \left[-\cos(L)\lambda_{P_1} + \sin(L)\lambda_{P_2} - 2\lambda_L\right]A_{R\_\text{pert}} + \lambda_L(\mu/a^2) \tag{11}$$

where $A_{\_\text{pert}}$ is the acceleration (computed numerically) due to the perturbation force. To simplify the Lagrange multipliers system, we omit the derivatives of the perturbations with respect to the state vector, whereas the Hamiltonian function is fully considered (because it does not contain any derivative). This simplification implies that the evolution of the auxiliary variable λ is different from the optimal case. We obtain the system

$$\lambda'_a = -2\lambda_a[(A_N + A_S)K_G + A_{T\_\text{pert}}] + 2\mu\lambda_L/a^3$$

$$\lambda'_{P_1} = 0, \qquad \lambda'_{P2} = 0, \qquad \lambda'_{Q_1} = 0, \qquad \lambda'_{Q2} = 0$$

$$\lambda'_L = -\left[2\cos(L)\lambda_{P_1} - 2\sin(L)\lambda_{P_2}\right][(A_N + A_S)K_G + A_{T\_\text{pert}}] - \left[\cos(L)\lambda_{Q_1} - \sin(L)\lambda_{Q_2}\right]\tfrac{1}{2}[(A_N - A_S)K + A_{W\_\text{pert}}] - \left[\sin(L)\lambda_{P_1} + \cos(L)\lambda_{P_2}\right]A_{R\_\text{pert}} \tag{12}$$

The performances are given in Table 4, and the thrust angle strategy for EITA S engine is shown in Fig. 7. The increase in inclination, subsequent to the perturbation forces, produces an increase in amplitude arcs, for configurations EITA S and N, from 90 (Keplerian case) to 120 deg.

In fact, with angles equal to the Keplerian case, the satellite gains the geostationary semi-axis with inclination greater than zero. To gain, at the same time, the geostationary values for the semi-axis and the inclination, the thrust arcs with EITA S and EITA N must increase, and consequently, the amplitude with EITA, with S and N components, must decrease. This fact increases the transfer time by about 20 days because the EITA S and N are less efficient at changing the semi-axis and need more revolutions to keep the geostationary altitude. This different thrust strategy does not change the consumption of mass, in fact, although the transfer time is longer, the satellite is using only one component (EITA S or EITA N) for longer time, and this balances the propellant expenditure.

As regards the thrust strategy, note two facts: First, the arc thrust, to change the inclination, is not central with respect to the nodal line, but begins 80 deg before, in a low-efficiency region for the Keplerian case. Second, in the last part of the transfer, like the Keplerian $+J_2$ case, the rotation of the argument of perigee is followed by rotation of the thrust arc for the EITA S engine (and also EITA N). In this case we have a big rotation of the argument of perigee, and we can see that the optimal thrust strategy, to change the inclination, takes into consideration the rotation of perigee and turns the arcs as much as possible but continues to contain the nodal line.

Comparison Between Simplified and Exact Optimization Process Considering only J_2 Effect

As in the preceding section, we simplify the system of Lagrange multipliers, but consider only the J_2 perturbation. The results are in Table 5 and the thrust angle strategy for the EITA S engine is in Fig. 8. The performances are similar to the exact case, thus showing that the simplification used does not affect the precision of results.

Optimization Process with Parametric Approach

A different way to approach the problem consists of using the method of parametric optimization where the variables are the amplitudes of the thrust arcs. We have four variables for the problem,

Table 4 Simplified case results all perturbations

Parameter	Value
Amplitude ascending node thrust, deg	−78, +44
Amplitude descending node thrust, deg	−78, +45
Inclination, deg	0.0058
Transfer time, days	189.4
Eccentricity	0.00005
Expended mass, kg	13.4

Table 5 Results including J_2 effect: simplified case

Parameter	Value
Amplitude ascending node thrust, deg	−48, +46
Amplitude descending node thrust, deg	−50, +46
Inclination, deg	0.0057
Transfer time, days	170.9
Eccentricity	0.000068
Expended mass, kg	13.4

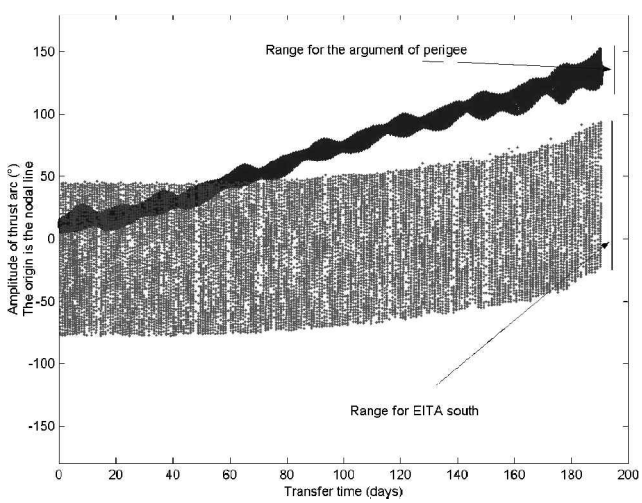

Fig. 7 Thrust strategy for EITA S: simplified case all perturbations.

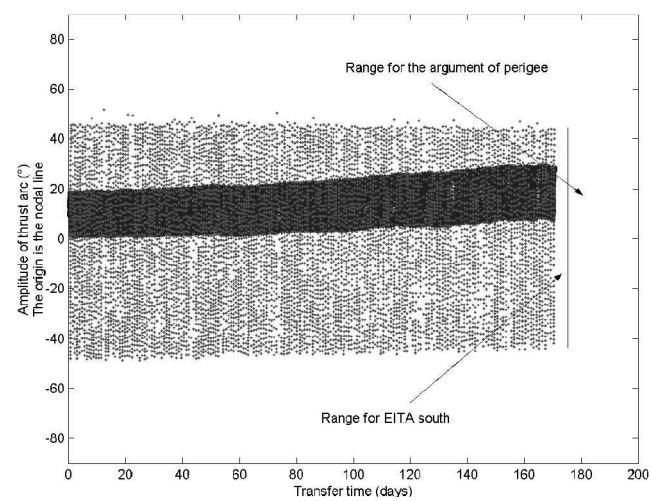

Fig. 8 Thrust strategy for EITA S including J_2 effect: simplified case.

Table 6 Parametric approach results

Parameter	Value
Amplitude ascending node thrust, deg	−78, +44.3
Amplitude descending node thrust, deg	−75, +44.4
Inclination, deg	0.0053
Transfer time, days	189.9
Eccentricity	0.000067
Expended mass, kg	13.4

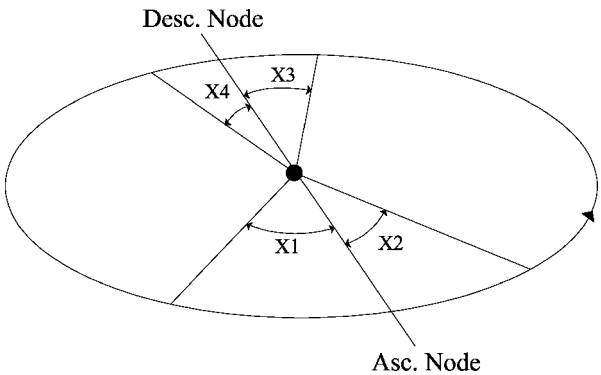

Fig. 9 Variables to optimizer.

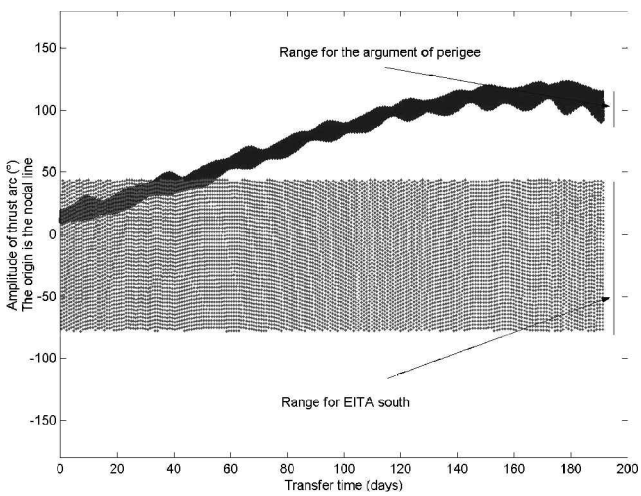

Fig. 10 Thrust strategy for EITA S: parametric approach.

corresponding to the amplitude thrust arcs around the nodal line (Fig. 9). The model for the simulation considers all perturbations. For this problem, the cost function is characterized by a large number of local minima very close to each other, and a computational effort must be made to find the best result. The best solution for the thrust arc amplitude value is found close to the value found using the Pontryagin theorem, but the transfer time is 0.5 days longer. This difference is because with the Pontryagin theorem the amplitudes of thrust arcs can change at every revolution and the control strategy becomes more efficient. When the parametric approach is used, this modulation on the control is possible only by using four variables for every revolution (about 760 variables in all), involving an enormous increase of computational effort. The performances of the transfer are given in Table 6, and the control strategy, for the EITA S engine, is shown in Fig. 10. The control, using only a few variables, is constrained to remain the same for all transfer times and cannot take into consideration possible variation of the argument of perigee, resulting, consequently, in less efficiency with respect to the Pontryagin case.

Conclusions

The minimum-time problem, for the transfer orbit of the Artemis satellite, is solved using the ion propulsion system and Pontryagin's principle. For the Keplerian case and for the Keplerian plus J_2 effect case, the full system for the Lagrange multipliers is considered, and the optimal strategy is found. The natural evolution of the orbital parameters implies that the effects of all perturbations must be considered in the simulation. Because of the increase of the complexity of the Lagrange multipliers, the derivatives of the perturbations with respect to the state are omitted in the Lagrange multipliers system. This simplification permits easy use of the minimum principle, in the case with perturbations, does not affect the precision of results, and it is very useful for computational purposes. In fact, the performance is better than that obtained with the parametric optimization approach.

Appendix: Multipliers Equations

When the J_2 effect is considered, the full expression for the Lagrange multipliers system is

$$\dot{\lambda}_a = -\Big\{2\lambda_a\big(A_{TM} + A_{TJ_2}\big) + \big[2a\lambda_a + 2\sin(L)\lambda_{P_1} + 2\cos(L)\lambda_{P_2}\big]\frac{\partial A_{TJ_2}}{\partial a} + \big[\sin(L)\lambda_{Q_1} + \cos(L)\lambda_{Q_2}\big]\frac{\partial A_{WJ_2}}{2\partial a} + \big[-\cos(L)\lambda_{P_1} + \sin(L)\lambda_{P_2} - 2\lambda_L\big]\frac{\partial A_{RJ_2}}{\partial a} - \frac{2\mu\lambda_L}{a^3}\Big\}$$

$$\dot{\lambda}_{P_1} = -\Big\{\big[2a\lambda_a + 2\sin(L)\lambda_{P_1} + 2\cos(L)\lambda_{P_2}\big]\frac{\partial A_{TJ_2}}{\partial P_1} + \big[\sin(L)\lambda_{Q_1} + \cos(L)\lambda_{Q_2}\big]\frac{\partial A_{WJ_2}}{2\partial P_1} + \big[-\cos(L)\lambda_{P_1} + \sin(L)\lambda_{P_2} - 2\lambda_L\big]\frac{\partial A_{RJ_2}}{\partial P_1}\Big\}$$

$$\dot{\lambda}_{P_2} = -\Big\{\big[2a\lambda_a + 2\sin(L)\lambda_{P_1} + 2\cos(L)\lambda_{P_2}\big]\frac{\partial A_{TJ_2}}{\partial P_2} + \big[\sin(L)\lambda_{Q_1} + \cos(L)\lambda_{Q_2}\big]\frac{\partial A_{WJ_2}}{2\partial P_2} + \big[-\cos(L)\lambda_{P_1} + \sin(L)\lambda_{P_2} - 2\lambda_L\big]\frac{\partial A_{RJ_2}}{\partial P_2}\Big\}$$

$$\dot{\lambda}_{Q_1} = -\Big\{\big[2a\lambda_a + 2\sin(L)\lambda_{P_1} + 2\cos(L)\lambda_{P_2}\big]\frac{\partial A_{TJ_2}}{\partial Q_1} + \big[\sin(L)\lambda_{Q_1} + \cos(L)\lambda_{Q_2}\big]\frac{\partial A_{WJ_2}}{2\partial Q_1} + \big[-\cos(L)\lambda_{P_1} + \sin(L)\lambda_{P_2} - 2\lambda_L\big]\frac{\partial A_{RJ_2}}{\partial Q_1}\Big\}$$

$$\dot{\lambda}_{Q_2} = -\Big\{\big[2a\lambda_a + 2\sin(L)\lambda_{P_1} + 2\cos(L)\lambda_{P_2}\big]\frac{\partial A_{TJ_2}}{\partial Q_2} + \big[\sin(L)\lambda_{Q_1} + \cos(L)\lambda_{Q_2}\big]\frac{\partial A_{WJ_2}}{2\partial Q_2} + \big[-\cos(L)\lambda_{P_1} + \sin(L)\lambda_{P_2} - 2\lambda_L\big]\frac{\partial A_{RJ_2}}{\partial Q_2}\Big\}$$

$$\dot{\lambda}_L = -\Bigg\{\Big[2\cos(L)\lambda_{P_1} - 2\sin(L)\lambda_{P_2}\Big]\big(A_{TM} + A_{TJ_2}\big)$$

$$+\Big[2a\lambda_a + 2\sin(L)\lambda_{P_1} + 2\cos(L)\lambda_{P_2}\Big]\frac{\partial A_{TJ_2}}{\partial L}$$

$$+\Big[\cos(L)\lambda_{Q_1} - \sin(L)\lambda_{Q_2}\Big]\frac{1}{2}\big(A_{WM} + A_{WJ_2}\big)$$

$$+\Big[\sin(L)\lambda_{Q_1} + \cos(L)\lambda_{Q_2}\Big]\frac{\partial A_{WJ_2}}{2\partial L}$$

$$+\Big[\sin(L)\lambda_{P_1} + \cos(L)\lambda_{P_2}\Big]A_{RJ_2}$$

$$+\Big[-\cos(L)\lambda_{P_1} + \sin(L)\lambda_{P_2} - 2\lambda_L\Big]\frac{\partial A_{RJ_2}}{\partial L}\Bigg\} \tag{A1}$$

Acknowledgments

The author gratefully acknowledges F. Graziani and P. Teofilatto for their comments and suggestions.

References

[1]Edelbaum, T. N., Sackett, L. L., and Malchow, H. L., "Optimal Low Thrust Geocentric Transfer," AIAA Paper 73-1074, Oct. 1973.

[2]Kluever, C. A., "Optimal Earth–Moon Trajectories Using Combined Chemical–Electric Propulsion," *Journal of Guidance, Control, and Dynamics*, Vol. 20, No. 2, 1997, pp. 253–258.

[3]Yamakawa, H., Kawaguchi, J., Uesugi, K., and Matsuo, H., "Frequent Access to Mercury in the Early 21st Century: Multiple Mercury Flyby Mission via Electric Propulsion," *Acta Astronautica*, Vol. 39, No. 1–4, 1996, pp. 133–142.

[4]Oleson, S. R., Myars, R. M., Kluever, C. A., Riehl, J. P., and Curran, F. M., "Advanced Propulsion for Geostationary Orbit Insertion and North–South Station-Keeping," AIAA Paper 95-2513, July 1995.

[5]Spitzer, A., "Near Optimal Transfer Orbit Trajectory Using Electric Propulsion," American Aeronautical Society, AAS Paper 95-215, Feb. 1995.

[6]Pierson, B. L., Kluever, C. A., "Three-Stage Approach to Optimal Low-Thrust Earth–Moon Trajectories," *Journal of Guidance, Control and Dynamics*, Vol. 17, No. 6, 1994, pp. 1275–1282.

[7]Chuang, C. H., Goodson, T. D., and Hanson, J., "Fuel-Optimal Low and Medium Thrust Orbit Transfers in Large Numbers of Burns," AIAA Paper 94-3650, Aug. 1994.

[8]Schwer, A. G., and Schoettle, U. M., "Transfer Mission Optimization of a Geostationary Spacecraft with a Solar Electric Arcject Propulsion System," AIAA Paper 94-3759, Aug. 1994.

[9]Cano, J. L., Hechler, M., Horas, D., Khan, M., Pulido, J., and Schoenmaekers, J., "SMART-1 Consolidated Report on Mission Analysis," ESA/ESOC, Rept. S1-ESC-RP-5506, Darmstadt, Germany, 16 July 2001.

[10]Noton, M., Salehi, S. V., and Elliot, C. A., "Navigation for Low Thrust Interplanetary Mission," ESA/ESOC, Final Report, ESA Contract No. 6209/85, Darmstadt, Germany, Oct. 1986.

[11]Pontryagin, L. S., Boltyanskii, V. G., Gamkrelidze, R. V., and Mishchenko, E. F., *The Mathematical Theory of Optimal Processes*, Pergamon Press, New York, 1964, pp. 19, 20.

[12]Geffroy, S., and Epenoy, R., "Optimal Low-Thrust Transfers with Constraints Generalization of Averaging Techniques," *Acta Astronautica*, Vol. 41, No. 3, 1997, pp. 133–149.

[13]Bryson, A. E., Jr., and Ho, Y.-C., *Applied Optimal Control*, Hemisphere, Washington, DC, 1975, pp. 108, 109.

[14]Marec, J.-P., *Optimal Space Trajectories*, Elsevier Scientific, Amsterdam, 1979, pp. 38, 39.

[15]Cefola, P. J. "Equinoctial Orbit Elements-Application to Artificial Satellite Orbits," AIAA Paper 72-937, Sept. 1972.

[16]Battin, R. H., *An Introduction to the Mathematics and Methods of Astrodynamics*, AIAA Education Series, AIAA, New York, 1987, pp. 490–493.

[17]Kechichian, J. A., "The Treatment of the Earth Oblateness Effect in Trajectory Optimization in Equinoctial Coordinates," *Acta Astronautica*, Vol. 40, No. 1, 1997, pp. 69–82.

[18]Kechichian, J. A., "Optimal Low-Earth-Orbit–Geostationary-Earth-Orbit Intermediate Acceleration Orbit Transfer," *Journal of Guidance, Control, and Dynamics*, Vol. 20, No. 4, 1997, pp. 803–811.

[19]Kechichian, J. A., "Minimum-Time Constant Accelerarion Orbit Transfer with First-Order Oblateness Effect," *Journal of Guidance, Control, and Dynamics*, Vol. 23, No. 4, 2000, pp. 595–603.

[20]Cochran, J. E., Jr., and Lee, S., "Optimal Low-Thrust Trajectories Using Equinotial Elements," International Astronautical Federation, Paper IAF-91-348, Oct. 1991.

[21]Conway, B. A., "Optimal Low-Thrust Interception of Earth-Crossing Asteroids," *Journal of Guidance, Control, and Dynamics*, Vol. 20, No. 5, 1997, pp. 995–1002.

[22]Rimrott, F. P. J., *Introductory Orbit Dynamics*, Vieweg, Brunswick, Germany, 1989, Chap. 5.